SUPPLEMENTARY DATA

MATERIALS AND METHODS

Complementary RNA (cRNA) labeling and hybridization for microarray

Quality and size distribution of RNA was assessed with an Agilent 2100 Bioanalyzer system using RNA 6000 Nano LabChip kit (Agilent Technologies, West Lothian, UK). 15 μg of total RNA was used to generate biotin-labeled cRNA using the Affymetrix one-cycle target labeling kit following the manufacturer's protocol (Affymetrix, High Wycombe, UK). Biotin-labeled cRNA was fragmented and hybridized to the Human Genome U133 plus 2.0 Array chips (Affymetrix). After hybridization, arrays were washed and processed using an Affymetrix Fluidic Station F450 following the manufacturer's instructions. The resulting GEM data have been submitted to the ArrayExpress data repository (www.ebi.ac.uk/arrayexpress) with accession number E-MEXP-2115. [Reviewers may access the data with username: Reviewer_E-MEXP-2115 and password: 1238580503164.]

Microarray Data Processing and Analysis Methods

Microarray Data Processing: Raw oligonucleotide probe-level data from 10 Affymetrix hgu133+2 GeneChip CEL files (5 CDC7-siRNA and 5 negative controls (Supplementary Figure 19)) were assessed for the presence or absence of specific signal at each of 54675 microarray probe-sets. Presence of specific signal was calculated using the default threshold ($p<0.04$) on the Affymetrix detection call statistic, as implemented in the affy toolbox of the Bioconductor suite of software (www.bioconductor.org) for the R statistical software package (www.R-project.org). The signals of 18794 probe-sets (34.37%) were found specific in all replicates of at least one experimental condition, and probe-level data of these probe-sets were background corrected, normalized and summarized using default parameters of the RMA model (Irizarry et al, 2003), as implemented in the Bioconductor affy

toolbox. The resulting data set contained processed log2 gene expression values for 10 samples across 18974 probe-sets.

Analysis of Differential Expression: In order to investigate changes in gene expression owing to *CDC7* knock-down, the moderated t-statistic (Smyth, 2004), implemented in the Bioconductor limma package, was applied to processed and filtered expression data to assess significance of differential gene (probe-set) expression between sample groups. In order to reduce errors associated with multiple hypothesis testing on such a scale, the significance p-values obtained were corrected by the family-wise error rate (FWER) method (Benjamini & Hochberg, 1995), as implemented in the Bioconductor multtest package. Probe-sets with corrected $p<0.01$ were deemed to exhibit significant differential expression between sample groups. At this threshold, 3779 microarray probe-sets were determined significantly differentially regulated.

Data Visualization: The dissimilarity between two microarray expression profiles of equal length was assessed with a bounded distance measure of (1.0 - Pearson correlation) (Supplementary Figure 20). Profiles were clustered for visualization using complete linkage hierarchical clustering, as implemented by the hclust function in the R statistics package. Heat maps of gene expression were created by importing relevant subsets of RNA processed microarray gene expression data into the dChipv1.3 microarray analysis package (www.biostat.harvard.edu/complab/dchip). In the case wherein a gene was represented by more than one probe-set on the array, a single probe-set was chosen to represent gene expression in the heat map according to highest mean expression over all samples (i.e. the most reliable sample hybridization regardless of group membership).

Over-representation Analysis: In order to investigate signaling pathways affected by the knock-down of *CDC7*, differentially regulated genes were analyzed according to their membership of KEGG (Kyoto

Encyclopedia of Genes and Genomes; www.genome.jp/kegg) pathways. Genes were annotated with the Bioconductor affy package. Hypergeometric statistics, implemented in the Bioconductor GOstats package, were employed to identify KEGG pathways over-represented within a gene subset of interest in comparison to their expected distribution across the entire GeneChip. A significance threshold of $p<0.05$ was employed to identify such categories.

REFERENCES

Benjamini Y, Hochberg Y (1995) Controlling the false discovery rate: a practical and powerful approach to multiple testing. *J R Statist Soc B* **57**: 289-300

Brunet A, Sweeney LB, Sturgill JF, Chua KF, Greer PL, Lin Y, Tran H, Ross SE, Mostoslavsky R, Cohen HY, Hu LS, Cheng HL, Jedrychowski MP, Gygi SP, Sinclair DA, Alt FW, Greenberg ME (2004) Stress-dependent regulation of FOXO transcription factors by the SIRT1 deacetylase. *Science* **303**: 2011-2015

Chen JH, Stoeber K, Kingsbury S, Ozanne SE, Williams GH, Hales CN (2004) Loss of proliferative capacity and induction of senescence in oxidatively stressed human fibroblasts. *J Biol Chem* **279**: 49439-49446

Choong ML, Yang H, Lee MA, Lane DP (2009) Specific activation of the p53 pathway by low dose actinomycin D: a new route to p53 based cyclotherapy. *Cell Cycle* **8**: 2810-2818

Crosio C, Fimia GM, Loury R, Kimura M, Okano Y, Zhou H, Sen S, Allis CD, Sassone-Corsi P (2002) Mitotic phosphorylation of histone H3: spatio-temporal regulation by mammalian Aurora kinases. *Mol Cell Biol* **22**: 874-885

Irizarry RA, Bolstad BM, Collin F, Cope LM, Hobbs B, Speed TP (2003) Summaries of Affymetrix GeneChip probe level data. *Nucleic Acids Res* **31**: e15

Machida YJ, Teer JK, Dutta A (2005) Acute reduction of an origin recognition complex (ORC) subunit in human cells reveals a requirement of ORC for Cdk2 activation. *J Biol Chem* **280**: 27624-27630

Montagnoli A, Tenca P, Sola F, Carpani D, Brotherton D, Albanese C, Santocanale C (2004) Cdc7 inhibition reveals a p53-dependent replication checkpoint that is defective in cancer cells. *Cancer Res* **64**: 7110-7116

Smyth GK (2004) Linear models and empirical bayes methods for assessing differential expression in microarray experiments. *Stat Appl Genet Mol Biol* **3**: Article3

SUPPLEMENTARY FIGURE LEGENDS

Supplementary Figure 1: *CDC7* knock-down in IMR90 fibroblasts causes reversible cell cycle arrest. (**A**) Transfection efficiency was determined for IMR90 cells cultured at low and high confluency levels using fluorescein-labeled random siRNA (green channel). Cells were fixed and double-stained with an anti-actin antibody (red channel). DNA was stained with DAPI (blue channel). (**B**) Three CDC7-siRNAs (oligos A and B (Montagnoli et al, 2004) and oligo V (validated by Ambion)) were tested by qRT-PCR for efficiency in knocking down CDC7 mRNA over a concentration range from 10 to 100 nM. Knock-down efficiency was defined as percentage (%) relative to control-siRNA (CO). All three oligos efficiently reduced CDC7 mRNA levels. (**C**) Each CDC7-siRNA was tested for efficiency to deplete Cdc7 protein in three replicates. Residual Cdc7 levels in whole cell extracts (WCE) were determined by western blot and compared with Cdc7 levels in WCE prepared from controls (UT: untreated cells, CO: control-siRNA, P: GAPDH-siRNA (positive control)). (**D**) Reproducibility of *CDC7* knock-down by oligo A was tested in four separate experiments comprising three replicates each. The significance (**) of the knockdown in each experiment was examined with one-way ANOVA ($p<0.001$). (**E**) WCE prepared from IMR90 cells transfected with control-siRNA (CO) and CDC7-siRNA 72 and 168 hours post-transfection were analyzed by immunoblotting with the indicated antibodies (β-actin – loading control). The ability of IMR90 cells to re-enter the cell cycle after Cdc7 levels had been restored is evident from (**F**) cell numbers in CO and Cdc7-depleted ($Cdc7^{KD}$) cell populations at the indicated times and (**G**) the degree of confluency at 168 hours compared to 72 hours post-transfection (phase contrast microscopy).

Supplementary Figure 2: **Specificity control for *CDC7* RNAi phenotype in IMR90 fibroblasts**. (**A**) CDC7 mRNA knock-down in IMR90 cells 72 hours post-transfection with an alternative CDC7-specific siRNA (oligo B) relative to cells transfected with control-siRNA (CO). (**B**) DNA content of

CO and $Cdc7^{KD}$ cells at 72 hours post-transfection. (**C**) Cytoplasmatic fractions (CF) and crude nuclear extracts (NE) prepared from CO and $Cdc7^{KD}$ (KD) cells (72 hours post-transfection) were analyzed by immunoblotting with the indicated antibodies (Orc4 – NE loading control; β-actin – CF loading control).

Supplementary Figure 3: **Expression of a *CDC7* gene variant refractory to silencing by CDC7-siRNA reverses cell cycle arrest in IMR90 cells**. (**A**) CDC7 mRNA expression in IMR90 cells transfected with CDC7-siRNA and a CDC7 rescue plasmid (R) relative to cells transfected with control-siRNA (CO) or CDC7-siRNA only. (**B**) DNA content of cells transfected with CO, CO plus R, CDC7-siRNA, and CDC7-siRNA plus R at 96 hours post-transfection. (**C**) At 96 hours post-transfection, cells were pulsed for 2 hours with BrdU, fixed and detected with a FITC-conjugated anti-BrdU antibody. DNA was stained with DAPI. Numbers show the percentage of cells incorporating BrdU. (**D**) Whole cell extracts (WCE) prepared from CO, CO plus R, CDC7-siRNA and CDC7-siRNA plus R transfected cells were analyzed by immunoblotting with the indicated antibodies (β-actin - loading control). (**E**) Cytoplasmatic fractions (CF) and crude nuclear extracts (NE) prepared from CO, CO plus R, CDC7-siRNA and CDC7-siRNA plus R transfected cells were analyzed by immunoblotting with the indicated antibodies (Orc4 – NE loading control; β-actin – CF loading control).

Supplementary Figure 4: Chk1 is not phosphorylated at Ser-345 after Cdc7 depletion in IMR90 cells. Crude nuclear extracts from untreated (UT), control-siRNA (CO) and CDC7-siRNA (KD) transfected IMR90 cells (72 hours post-transfection), and from untreated (UT) and hydroxyurea treated (4 hours, 3 mM HU) U2OS cells were analyzed by immunoblotting with anti-phospho serine 345 (pS345) Chk1 antibody (β-actin – loading control).

Supplementary Figure 5: **Heat-maps based on GEM analysis of IMR90 cells transfected with CDC7-siRNA and control-siRNA**. (**A**) Cell cycle related-, (**B**) p53- and (**C**) Wnt-signaling pathways are the most significantly affected cell proliferation-associated signaling pathways after Cdc7 depletion (84 hours post-transfection). The maps display microarray data (5 CDC7-siRNA and 5 negative control experiments) corresponding to differentially-expressed pathway genes, with expression standardized to have zero mean and unit standard deviation across samples. The color-scale displays over- and under-regulation (shades of red and blue respectively) in units of standard deviation from mean expression across samples.

Supplementary Figure 6: **Cell cycle arrest following Cdc7 depletion is p53-dependent.** (**A**) Crude nuclear extracts (NE) prepared from untreated (UT), control-siRNA (CO) and CDC7-siRNA (KD) transfected IMR90 cells (96 hours post-transfection) were analyzed by immunoblotting with the indicated antibodies (Orc4 – loading control). (**B**) At the same time point CO and $Cdc7^{KD}$ cell populations were fixed and ARF protein was detected by indirect immunofluorescence with an anti-$p14^{ARF}$ antibody and fluorescein-labeled secondary antibody. DNA was stained with DAPI. (**C**) WCE prepared from $Cdc7^{KD}$, $Cdc7^{KD}$/$p53^{KD}$, CO and $p53^{KD}$/CO cells (96 hours post-transfection) were analyzed by immunoblotting with the indicated antibodies. The data show downregulation of p53 in doubly-depleted Cdc7/p53 cells to baseline levels seen in control cells, which in turn resulted in p21 downregulation. The increase in cyclin B levels and histone H3 Ser-10 phosphorylation (Crosio et al, 2002) indicate that doubly-depleted Cdc7/p53 cells appear to be unable to trigger a checkpoint response to Cdc7 depletion, instead progressing towards the G2/M boundary. (**D**) DNA content of $Cdc7^{KD}$ and doubly-depleted Cdc7/p53 ($Cdc7^{KD}$/$p53^{KD}$) cells was determined at the indicated time points. The sharp decline in the G2/M population in doubly-depleted Cdc7/p53 cells 96 hours post-transfection and concomitant increase in the number of cells with less than 2C DNA content suggest that failure to elicit the Cdc7-depletion induced checkpoint leads to apoptotic cell death. (**E**) WCE from $Cdc7^{KD}$,

$Cdc7^{KD}/p53^{KD}$, CO, and $p53^{KD}/CO$ cells were analyzed by immunoblotting with the indicated antibodies. Detection of caspase 3 activation and PARP-1 cleavage confirms induction of apoptosis in doubly-depleted Cdc7/p53 cells. Note that while some PARP cleavage and caspase 3 activation were also evident in control- plus p53-siRNA transfections, the intensities of the bands for the p85 and p17 cleavage products were 3-fold and 7-fold lower compared to doubly-depleted Cdc7/p53 cells (Image J densitometry analysis). (**F**) Cell death and fragmented apoptotic nuclei (inset) were detected by phase contrast and fluorescent microscopy in doubly-depleted $Cdc7^{KD}/p53^{KD}$ cells, but not in $Cdc7^{KD}$ cells. DAPI was used to stain DNA. (**G**) Cytoplasmatic protein fractions (CF) from CO and $Cdc7^{KD}$ cells (84 hours post-transfection) and from $Cdc7^{KD}/p53^{KD}$ cells (72 and 84 hours post-transfection) were analyzed by immunoblotting with Dkk3 antibody (β-actin – loading control).

Supplementary Figure 7: ***HDM2* gene expression**. HDM2 mRNA levels in IMR90 fibroblasts transfected with CDC7-siRNA ($Cdc7^{KD}$) relative to cells transfected with control-siRNA (CO) at 72, 96 and 120 hours post-transfection.

Supplementary Figure 8: **Double-knockdown experiments in IMR90 cells using CDC7, P53-, DKK3-, CDKN2B/p15 and FOXO3A siRNAs**. 72 hours after CDC7-siRNA transfection, cells were replated at low density and transfected with either CDC7- (10 nM) and control-siRNA (10 nM), or (**A**) CDC7- (10 nM) and p53-siRNA, or (**B**) CDC7-siRNA (10nM) and a cocktail of two DKK3-siRNAs (each 10 nM), or (**C**) CDC7- (10nM) and FOXO3A-siRNA (10 nM), or (**D**) CDC7- (10nM) and a cocktail of CDKN2B/p15-siRNAs 1, 2 and 3 (each 5 nM). Cdc7 downregulation in single- and double knock-downs was confirmed for each experiment (not shown). The efficiency of double knock-downs was determined by qRT-PCR and is shown relative to the mRNA level in Cdc7-depleted cells (set as 100%).

Supplementary Figure 9: **Cdk2 activity is restored in doubly-depleted Cdc7/p53 IMR90 cells**. WCE prepared from control-siRNA (CO) and CDC7-siRNA ($Cdc7^{KD}$) transfected IMR90 cells and from doubly-depleted $Cdc7^{KD}/p53^{KD}$ cells were analyzed by immunoblotting with the indicated antibodies (β-actin – loading control). Note that Ser-53 of the N-terminal tail of Mcm2 is a mapped Cdc7-specific phosphosite, whereas Ser-27 is a Cdk2-specific phosphosite.

Supplementary Figure 10: **Dickkopf 3 (Dkk3) protein is N-glycosylated in IMR90 fibroblasts**. (**A**) WCE prepared from control-siRNA (CO) and CDC7-siRNA ($Cdc7^{KD}$) transfected cells were analysed by immunoblotting with Dkk3 antibody alone (Ab; lanes 1 and 2) or Dkk3 antibody preincubated with recombinant Dkk3 blocking peptide (pep, 1:1 w/w) (β-actin – loading control). Note that preincubation abolished detection of the different bands recognized by the Dkk3 antibody, suggesting the presence of Dkk3 isoforms. (**B**) Cytoplasmatic protein fractions (CF) prepared from CO and $Cdc7^{KD}$ cells were digested with N-glycanase and analysed by immunoblotting with Dkk3 antibody. Note that the product of the N-glycanase reactions (lanes 2 and 5: partial digestion; lanes 3 and 6: complete digestion) shows a decreased molecular weight in comparison to undigested extract, indicating that the reduction in molecular weight is due to removal of N-linked oligosaccharides from the Dkk3 polypeptide backbone. (**C**) CF prepared from CO and $Cdc7^{KD}$ cells and from doubly-depleted $Cdc7^{KD}/Dkk3^{KD}$ cells 72 and 96 hours post-transfection were immunoblotted with Dkk3 antibody. Note that at the later time point (96 hours) *DKK3* knock-down in the Cdc7-depleted background abolishes immunodetection of all Dkk3 isoforms, reinforcing the specificity of the Dkk3 antibody.

Supplementary Figure 11: **Dkk3 and Wnt-signalling components in IMR90 fibroblasts arrested through specific activation of the p53 pathway by low dose actinomycin D**. Low dose treatment with actinomycin D (ActD) at 1 nM has been shown to mimic the HDM2 inhibitor nutlin-3 in the

highly specific activation of p53-dependent transcription and induction of a reversible cell cycle arrest in normal cells (Choong et al, 2009). ActD's more commonly known DNA damaging and RNA synthesis inhibition effects are generated only at higher dosage (100-200 nM). To determine whether p53-dependent inducible Dkk3 expression in response to *CDC7* knock-down (Figure 3; Supplementary Figures 5 and 6) is closely associated with origin firing or, alternatively, part of a common p53-induced cell cycle arrest pathway, the expression dynamics of p53-pathway and Wnt-signaling components including Dkk3 were compared in Cdc7-depleted and ActD-treated (1 nM) IMR90 fibroblasts. (**A**) DNA content of control-siRNA (CO) and CDC7-siRNA ($Cdc7^{KD}$) transfected IMR90 cells (72 hours post-transfection) and DMSO- and ActD-treated cells (24 hour treatment). Cell cycle arrest in $Cdc7^{KD}$ and ActD cells compared to CO and DMSO-treated cells, respectively, is demonstrated by the reduction of cells in S phase and concomitant increase of cells in G1 phase. (**B**) DKK3 isoform A, DKK3 isoform B, CDKN1A (p21) and HDM2 mRNA levels in $Cdc7^{KD}$ and ActD cells were determined by qRT-PCR and are shown in comparison with mRNA levels in CO cells and DMSO-treated cells. DKK3 isoform A and B transcript levels increased two-fold and four-fold in $Cdc7^{KD}$ cells relative to CO cells, whereas levels of both mRNA isoforms decreased after ActD-treatment. Activation of the p53 pathway is confirmed by a 4-fold increase in p21 transcript levels in Cdc7-depleted cells, and 4-fold and 3-fold increases in p21 and HDM2 mRNA levels in ActD cells. (**C**) Crude cytoplasmatic fractions (CF) and nuclear extracts (NE) prepared from CO and $Cdc7^{KD}$ cells and from DMSO-treated and ActD cells were analyzed by immunoblotting with the indicated antibodies (Orc4 – NE loading control; β-actin – CF loading control). Whilst p53 protein was stabilized and p21 levels raised in both $Cdc7^{KD}$ and ActD cells, the inducible, faster migrating Dkk3 isoform and a marked reduction in nuclear β-catenin and cyclin D1 levels were only detectable in Cdc7-depleted cells. These data argue against p53-dependent DKK3 upregulation being part of a common cell cycle

arrest pathway and support a more intimate connection between inducible Dkk3 expression and DNA replication control.

Supplementary Figure 12: **DNA content of IMR90 fibroblasts**. Flow cytometric analyses of IMR90 cells transfected with (**A**) control-siRNA (CO), (**B**) CDC7-siRNA ($Cdc7^{KD}$), and co-transfected with (**C**) CDC7/DKK3 and (**D**) CDC7/p15 siRNAs.

Supplementary Figure 13: FoxO3a mediates expression of *CDKN2A/ARF*, *CDKN2B/p15* and *CDKN1B/p27* in Cdc7-depleted IMR90 cells. (**A**) CDKN2A/ARF, CDKN2B and CDKN1B mRNA levels in $Cdc7^{KD}$ cells were determined by qRT-PCR and are shown in comparison with mRNA levels in CO cells. (**B**) CDKN2A/ARF, CDKN2B and CDKN1B mRNA expression in CO and doubly-depleted $Cdc7^{KD}$/$FoxO3a^{KD}$ cells was measured by qRT-PCR and compared with $Cdc7^{KD}$ cells (set as 100%).

Supplementary Figure 14: **Protein levels of origin activation checkpoint components in G1 phase fibroblasts**. The observed changes in the protein levels of origin activation checkpoint components could be indirect consequences of cell cycle position. To exclude this possibility, two different approaches were used to prepare G1 phase populations of control-transfected (CO) IMR90 cells and checkpoint protein levels in these G1 cells were compared to those in Cdc7-depleted ($Cdc7^{KD}$) cells. (**A**) A synchronous population of CO cells was obtained after release from double-thymidine block (DTB) and transfection with control-siRNA. Progression into G1 was monitored by flow cytometry and entry into the subsequent S phase (between 25 and 27 hours after the release) determined by BrdU incorporation (insets; numbers show the percentage of cells incorporating BrdU). (**B**) Whole cell extracts (WCE) prepared from asynchronous untreated cells (UT), CO cells at the G1-S boundary (25 hours after release from DTB) and $Cdc7^{KD}$ cells were analyzed by immunoblotting with the indicated

antibodies (β-actin – loading control). Notably, increased FoxO3a levels, the inducible faster migrating Dkk3 isoform, and increased protein levels of ARF, p53 and the CDK inhibitors p15, p21 and p27 are evident in Cdc7-depleted cells. (**C**) G1 cell fractions of CO and $Cdc7^{KD}$ cells were obtained by one-way sorting of propidium iodide stained cells with a DAKO/Beckman Coulter MoFlo High Speed Sorter. Flow cytometry profiles generated pre- and post-sorting demonstrate the purity of the G1 phase cell populations. Western blot analysis of WCE prepared from G1 cell fractions of CO and $Cdc7^{KD}$ cells confirms that the changes in checkpoint protein levels are caused by Cdc7-depletion and are not an indirect consequence of cell cycle position.

Supplementary Figure 15: Regulation of origin activation checkpoint components in oxidatively stressed IMR90 fibroblasts. FoxO transcription factors are regulated by a wide range of stimuli including reactive oxygen species (Brunet et al, 2004). To determine whether the cellular responses elicited by FoxO3a in response to *CDC7* knock-down are specific to origin firing or, alternatively, part of a general FoxO-dependent gene expression program, the expression dynamics of checkpoint components were compared in Cdc7-depleted and oxidatively stressed IMR90 fibroblasts. IMR90 cells were stressed twice for two hours with 600 μM H_2O_2 as previously described (Chen et al, 2004). (**A**) DNA content of untreated (UT) and oxidatively stressed (H_2O_2-treated) IMR90 cells. Compared to untreated cells, cell cycle arrest in the H_2O_2-treated cells is demonstrated by the reduction of cells in S phase and the increase of cells in G1 phase. (**B**) Crude nuclear extracts (NE) and cytoplasmatic fractions (CF) prepared from UT, H_2O_2-treated and from control-siRNA (CO) and CDC7-siRNA transfected ($Cdc7^{KD}$) cells were analyzed by immunoblotting with the indicated antibodies (Orc4 – NE loading control; β-actin – CF loading control). The western blot data show that oxidative stress stimuli increased FoxO3a protein levels and allowed FoxO3a to enter the nucleus. Nuclear accumulation of FoxO3a was also seen, albeit to a lesser extent, in Cdc7-depleted cells. Both oxidative stress and Cdc7-

depletion caused an increase in p53 levels and induction of p21. Of the FoxO3a target genes studied, ARF protein expression was markedly increased only in Cdc7-depleted cells, whereas p15 and p27 levels were raised in cells arrested by either oxidative stress or *CDC7* knock-down. Notably, the inducible, faster migrating Dkk3 isoform was also only detectable in Cdc7-depleted cells. Thus while p15 and p27 upregulation in both oxidatively stressed and Cdc7-depleted fibroblasts indicates that these axes of the origin activation checkpoint overlap with a common FoxO-induced cell cycle arrest pathway, inducible ARF and Dkk3 expression are more specific events associated with DNA replication control.

Supplementary Figure 16: **Single knock-downs of origin activation checkpoint components in IMR90 fibroblasts**. Knock-down of individual components of the origin activation checkpoint in IMR90 cells previously arrested by Cdc7-depletion bypasses the cell cycle arrest (Figures 3-5; Supplementary Figure 6). To exclude the possibility that p53, Dkk3, FoxO3a or p15 depletion can cause strong S phase stimulation on their own, IMR90 cells were first transfected with control-siRNA and after 72 hours replated at low density and transfected with either control-siRNA (CO), control- and p53-siRNAs ($p53^{KD}$), or control and DKK3 ($Dkk3^{KD}$) or FOXO3A ($FoxO3a^{KD}$) or CDKN2B ($p15^{KD}$) oligos. (**A**) Flow cytometry profiles, cell cycle phase distribution data (numbers in pie charts represent the percentage of cells in G1 phase, S phase and G2/M), target mRNA levels in percent relative to control, and western blots of target proteins (insets) are shown for each of the single knock-downs and compared with untreated (UT) and CO cells. (**B**) Whole cell extracts prepared from CO, $p15^{KD}$, $p53^{KD}$, $Dkk3^{KD}$ and $FoxO3a^{KD}$ cells were analyzed by immunoblotting with the indicated antibodies (β-actin – loading control). The flow cytometry profiles and cell cycle phase distribution data demonstrate that single knock-downs of the studied checkpoint components do not cause strong S phase stimulation on their own. This is further supported by the western blot data which show no significant increase in protein levels of the S/G2 phase markers cyclin A and geminin. Caspase 3 activation and PARP-1

cleavage were also not detected, indicating that single depletions of these checkpoint components do not cause apoptosis in this experimental system.

Supplementary Figure 17: **Cdc7-depletion induced cell cycle arrest in WI-38 fibroblasts**. In this study the cellular response to Cdc7 depletion has been investigated in IMR90 cells. To control for the possibility that the discovered cell cycle arrest phenotype is specific to the IMR90 strain, the main study findings were reproduced in a different strain. (**A**) DNA content of untreated (UT), control-siRNA (CO) and CDC7-siRNA ($Cdc7^{KD}$) transfected WI-38 fibroblasts (72 hours post-transfection). (**B**) Crude cytoplasmatic fractions (CF) and nuclear extracts (NE) prepared from untreated, CO and $Cdc7^{KD}$ WI-38 cells were analyzed by immunoblotting with the indicated antibodies (Orc4 – NE loading control; β-actin – CF loading control). The flow cytometry data show that *CDC7* knock-down in WI-38 cells caused the same shifts in cell cycle phase distribution as Cdc7-depletion in IMR90 cells (Figure 1D), with cell cycle arrest evident from the large reduction of cells in S phase and the increase of cells in G1 phase. As seen in Cdc7-depleted IMR90 cells, *CDC7* knock-down in WI-38 cells resulted in FoxO3a nuclear accumulation, increased ARF and p53 protein levels, the appearance of the inducible, faster migrating Dkk3 isoform, and increased levels of the CDK inhibitors p15, p21 and p27. Low CDK activity in the Cdc7-depleted WI-38 cells was confirmed by the significant reduction in Mcm2 phosphorylation at the CDK phosphosite Ser-27. Thus the cell cycle arrest phenotype first discovered in IMR90 fibroblasts is fully reproducible in WI-38 cells in response to *CDC7* knock-down, arguing against the possibility that the Cdc7-depletion induced checkpoint response could be strain specific.

Supplementary Figure 18: ***ORC2* knock-down causes a cell cycle arrest phenotype in IMR90 cells strongly reminiscent of Cdc7-depleted cells**. (**A**) ORC2 mRNA knock-down ($Orc2^{KD}$) in IMR90 cells relative to cells transfected with control-siRNA (CO). (**B**) DNA content of CO and $Orc2^{KD}$ cells at 72

hours post-transfection. (**C**) Crude nuclear extracts (NE) and cytoplasmatic fractions (CF) prepared from CO and ORC2-siRNA ($Orc2^{KD}$) transfected cells were analyzed by immunoblotting with the indicated antibodies (Orc4 and β-actin – loading controls).

Supplementary Figure 19: **Analysis of RNA samples by qRT-PCR prior to microarray hybridization**. IMR90 cells were transfected with specific CDC7-siRNA for 84 hours and RNA was extracted. From 8 RNA sample preparations 6 (*) were chosen for microarray hybridization based on knock-down score as determined by qRT-PCR.

Supplementary Figure 20: Hierarchical clustering of transcriptional profiles. Complete-linkage hierarchical clustering of filtered and processed microarray profiles. The dissimilarity between two microarray expression profiles of equal length was assessed with a bounded distance measure of (1.0 - Pearson correlation) (y-axis).

SUPPLEMENTARY TABLES

Supplementary Table 1: Sequences of sense and antisense siRNA oligonucleotides

Target	(5'→3') sense oligo	Antisense oligo
CDC7-A*	GCUCAGCAGGAAAGGUGUUUU	AACACCUUUCCUGCUGAGCUU
CDC7-B*	GCAGUCAAAGACUGUGGAUUU	AUCCACAGUCUUUGACUGCUU
CDC7-V	GGCUGAAGGCUCUUUAAAAtt	UUUUAAAGAGCCUUCAGCCtg
p53*	GGAAGACUCCAGUGGUAAUUU	AUUACCACUGGAGUCUUCCUU
CDKN2B†	GCAAUUGUAACGGUUAACUtt	AGUUAACCGUUACAAUUGCtc
CDKN2B†	GCCUGUCUGAGACUCACAGtt	CUGUGAGUCUCAGACAGGCtt
CDKN2B#	CCCACCUAAUUCGAUGAAGtt	CUUCAUCGAAUUAGGUGGGtg
ORC2L‡	AAGAAGGAGCGAGCGAGCGCAGCUU	UUUUCUUCCUCGCUCGCUCGCGUCG

* CDC7-A, -B and p53 sequences from Montagnoli et al, 2004
‡ ORC2L sequence from Machida et al, 2005
† predesigned
# validated

Supplementary Table 2: **Signaling pathway over-representation analysis**. Differentially regulated genes were analyzed according to their membership of KEGG (Kyoto Encyclopedia of Genes and Genomes; www.genome.jp/kegg) pathways. Hypergeometric statistics were employed to identify KEGG pathways over-represented within the subset of differentially regulated genes in comparison to their expected distribution across the entire GeneChip. A significance threshold of $p<0.05$ was employed to identify such categories.

KEGG ID	Term	Size	Markers	Expected	p-value
hsa4115	**p53 signaling pathway**	**68**	**32**	**11.79**	**1.07E-08**
hsa4110	**Cell cycle**	**112**	**36**	**19.42**	**7.87E-05**
hsa4510	Focal adhesion	194	51	33.63	8.74E-05
hsa4520	Adherens junction	76	23	13.18	3.66E-03
hsa4130	SNARE interactions in vesicular transport	36	13	6.24	5.30E-03
hsa4810	Regulation of actin cytoskeleton	204	48	35.36	0.013
hsa4310	**Wnt signaling pathway**	**146**	**36**	**25.31**	**0.014**
hsa4360	Axon guidance	128	32	22.19	0.017
hsa4120	Ubiquitin mediated proteolysis	45	14	7.80	0.017
hsa4530	Tight junction	117	29	20.28	0.024
hsa4012	ErbB signaling pathway	87	22	15.08	0.038
hsa4340	Hedgehog signaling	55	15	9.53	0.043
hsa4210	Apoptosis	84	21	14.56	0.046
hsa4370	VEGF signaling	70	18	12.14	0.049

Supplementary Table 3: Sequences of primers used for qRT-PCR

Target	Primer pair
CDC7	5'-AACTTGCAGGTGTTAAAAAAG-3'
	5'-TGAAAGTGCCTTCTCCAAT-3'
p53	5'-TGAGGTTGGCTCTGACTGTA-3'
	5'-AGATTACCACTGGAGTCTTCC-3'
DKK3 (isoform A)	5'-GTGGAAGAGATGGAGGCAGA-3'
	5'-TTGGTTATCTTGTGAATTTCTCG-3'
DKK3 (isoform B)	5'-TGGAAGAGATGGAGGCAGAA-3'
	5'-TTGGTTATCTTGTGAATTTCTCG-3'
p15INK4B (CDKN2B)	5'-GCGGGGACTAGTGGAGGA-3'
	5'-CATCATCATGACCTGGATCG-3'
FOXO3A	5'-CGTAGTGAACTCATGGATGC-3'
	5'-ACTTCCCCTTCCTCAGTGAT-3'
ORC2L	5'-CCAGCTGGACAACCAGGATA-3'
	5'-GCTTTGGTCTAACCAGGGTCT-3'
HDM2	5'-GAGCAGGCAAATGTGCAATA-3'
	5'-GCTTTGGTCTAACCAGGGTCT-3'
GAPDH	5'-TCAACTACATGGTTTACATGTTC-3'
	5'-GATCTCGCTCCTGGAAGAT-3'

Supplementary Figure 1

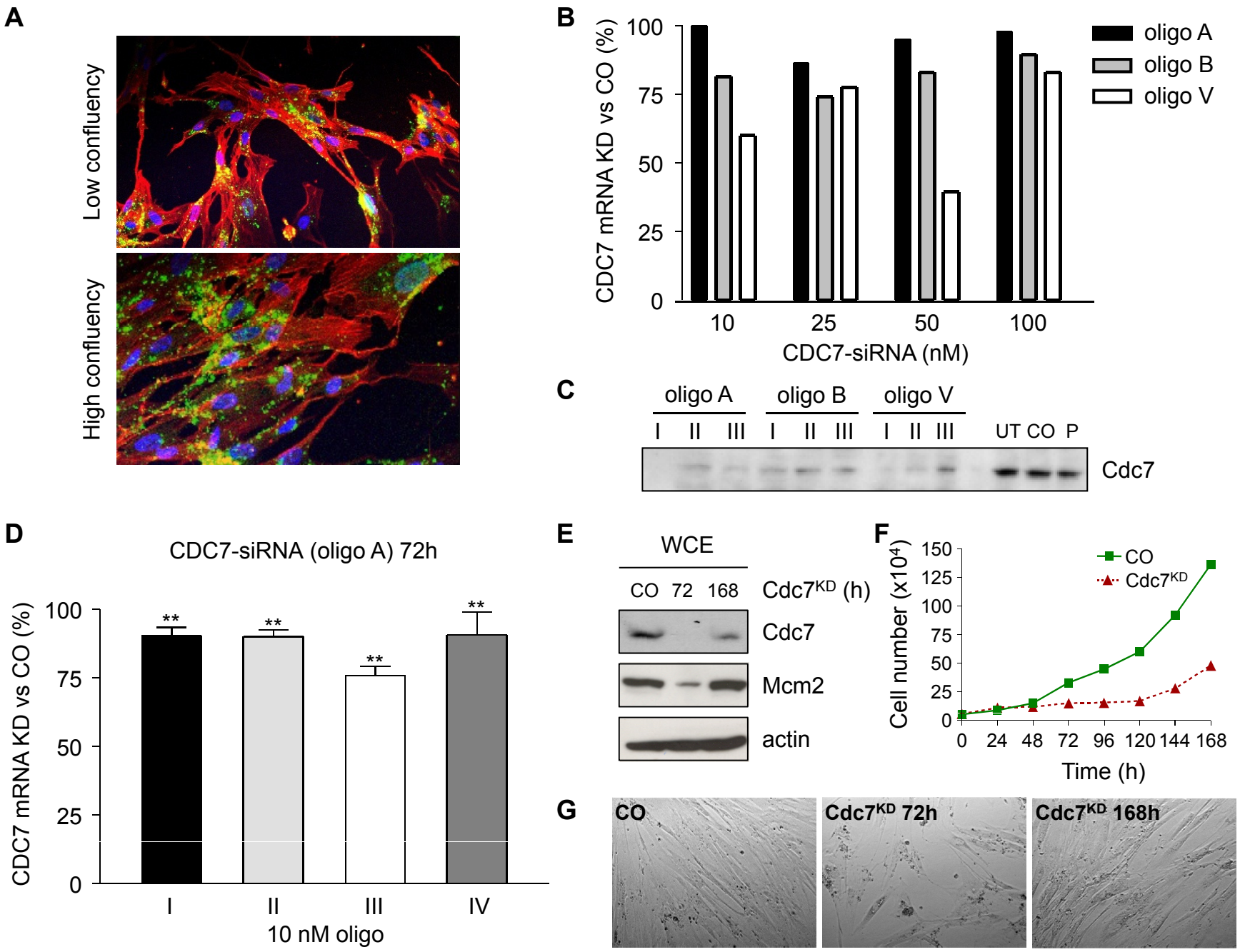

Supplementary Figure 2

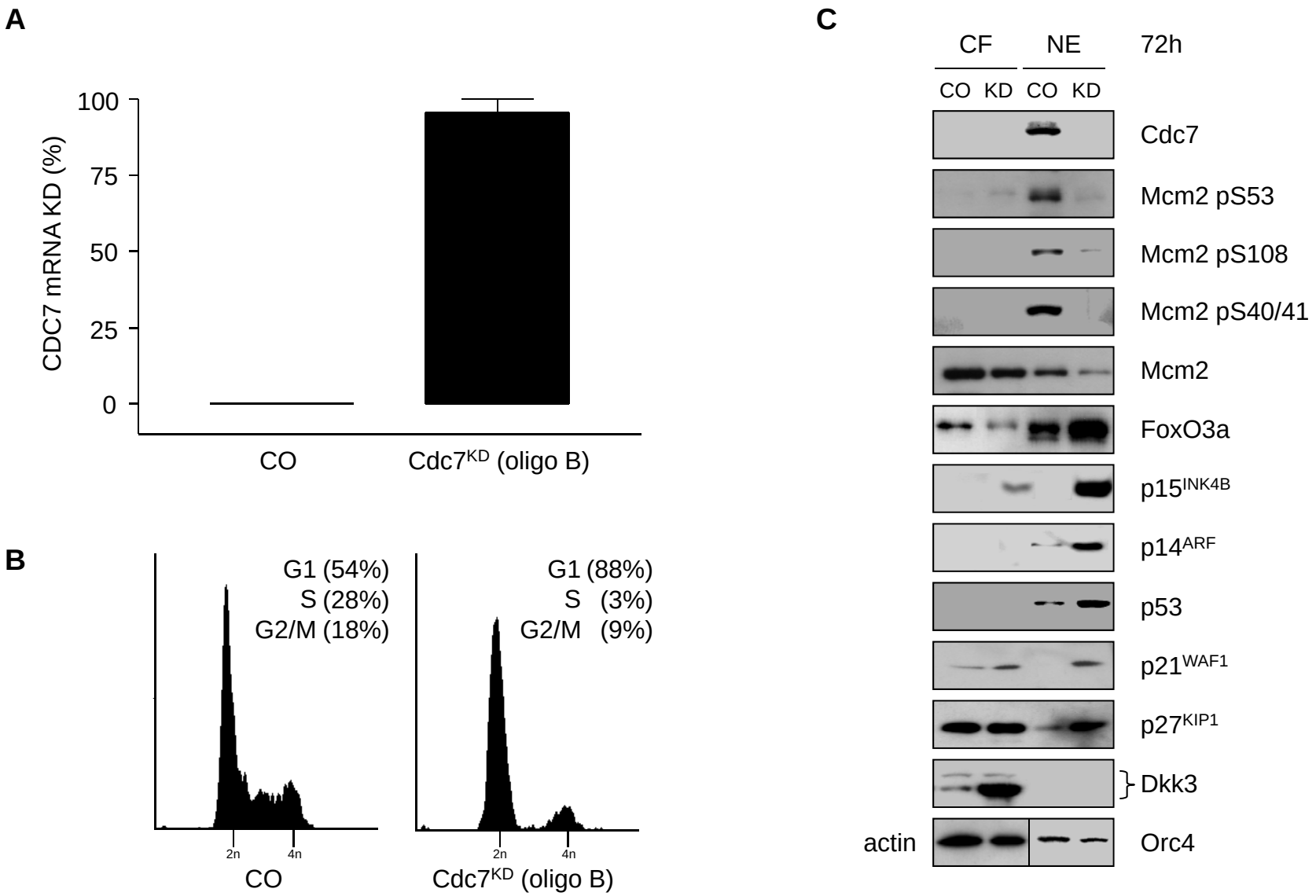

Supplementary Figure 3

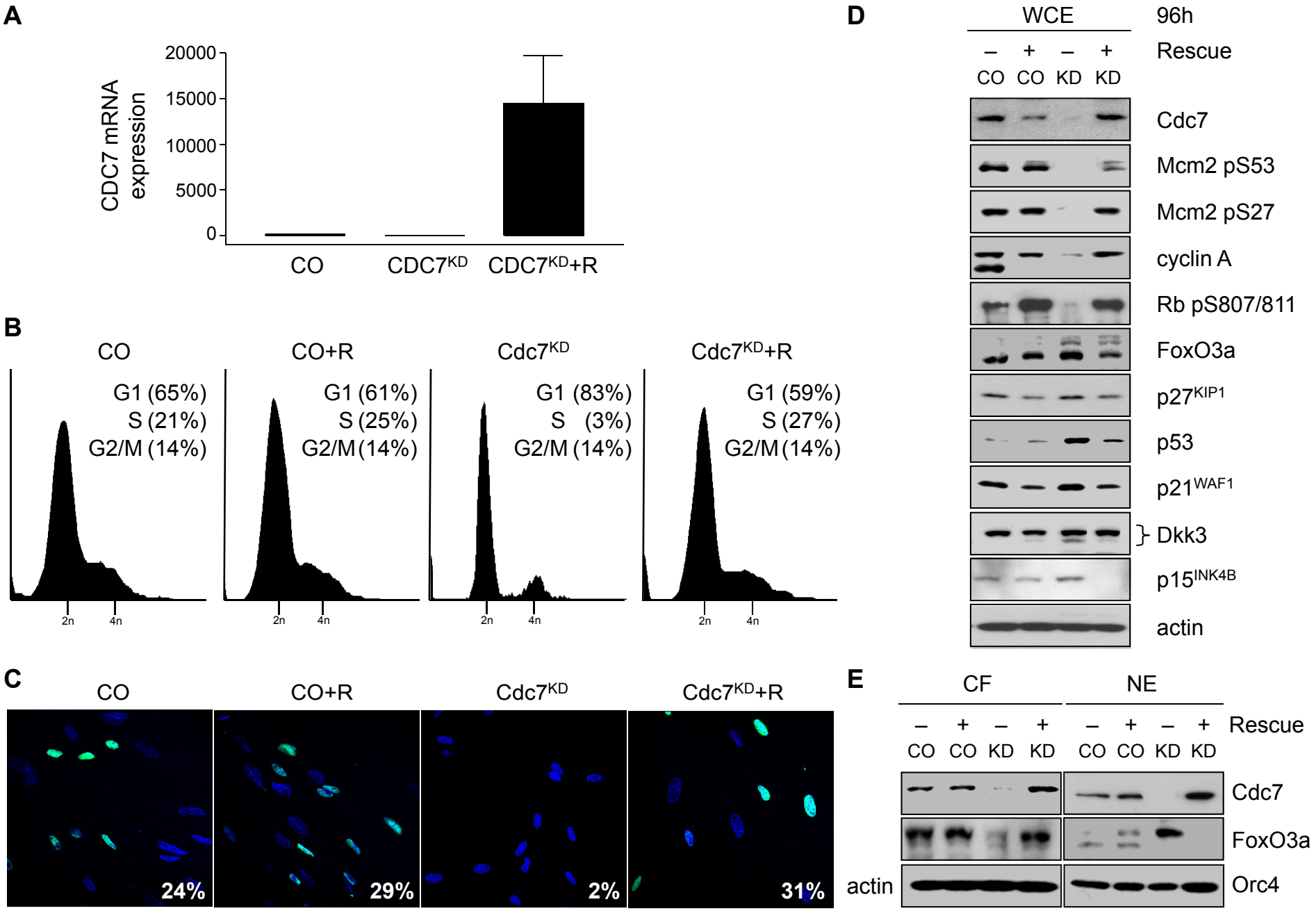

Supplementary Figure 4

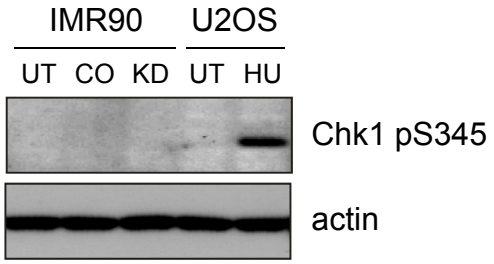

Supplementary Figure 5

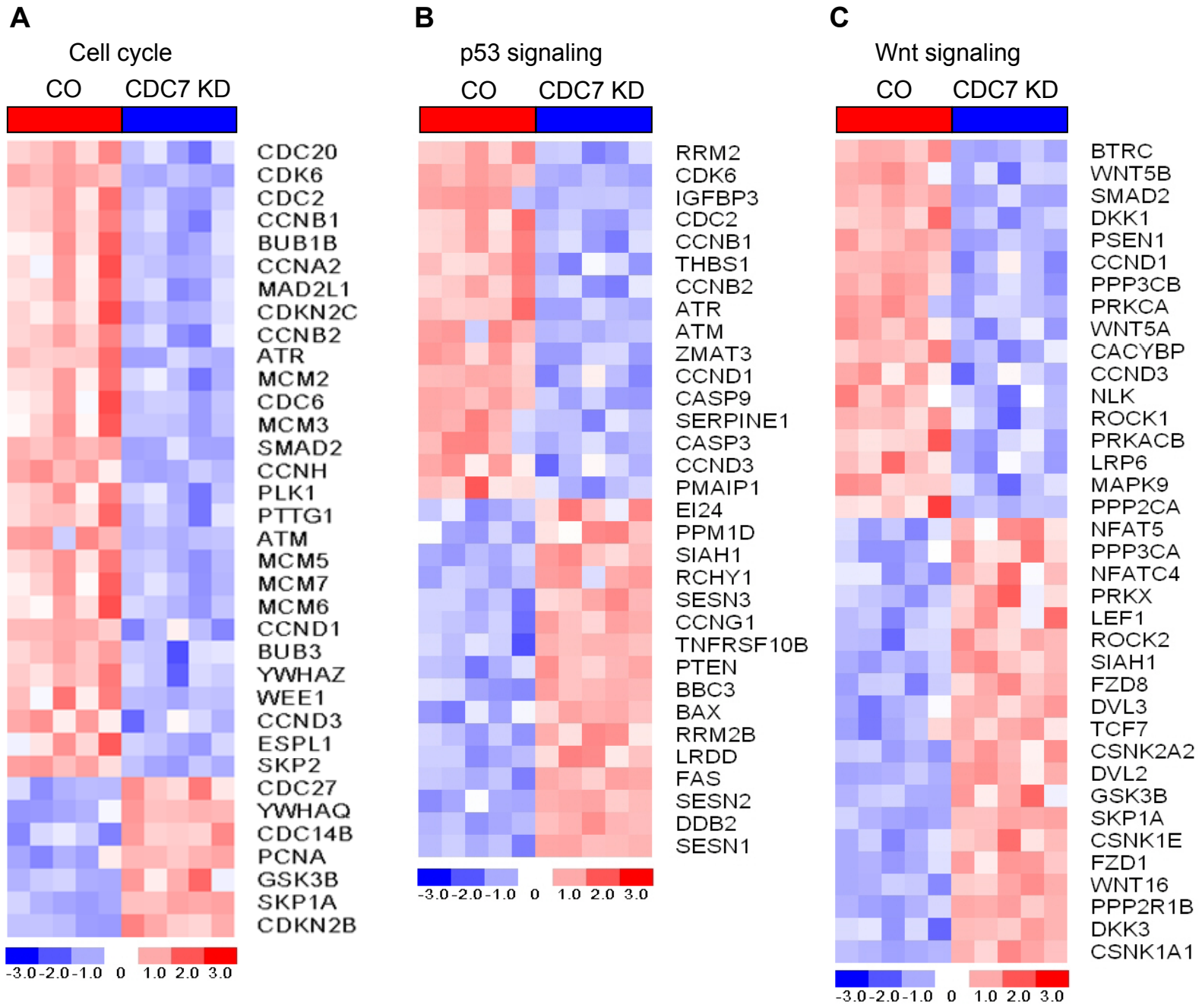

Supplementary Figure 6

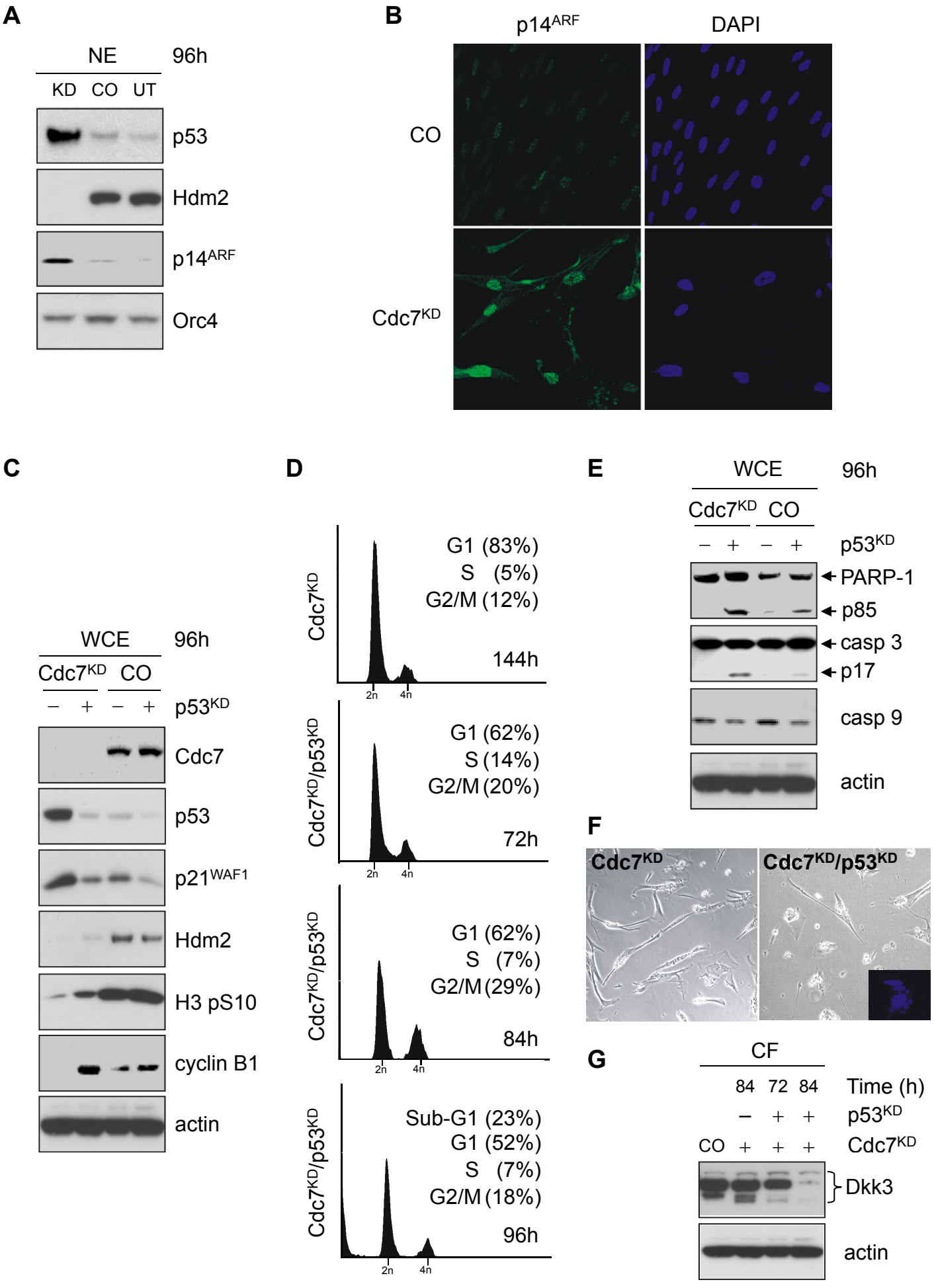

Supplementary Figure 7

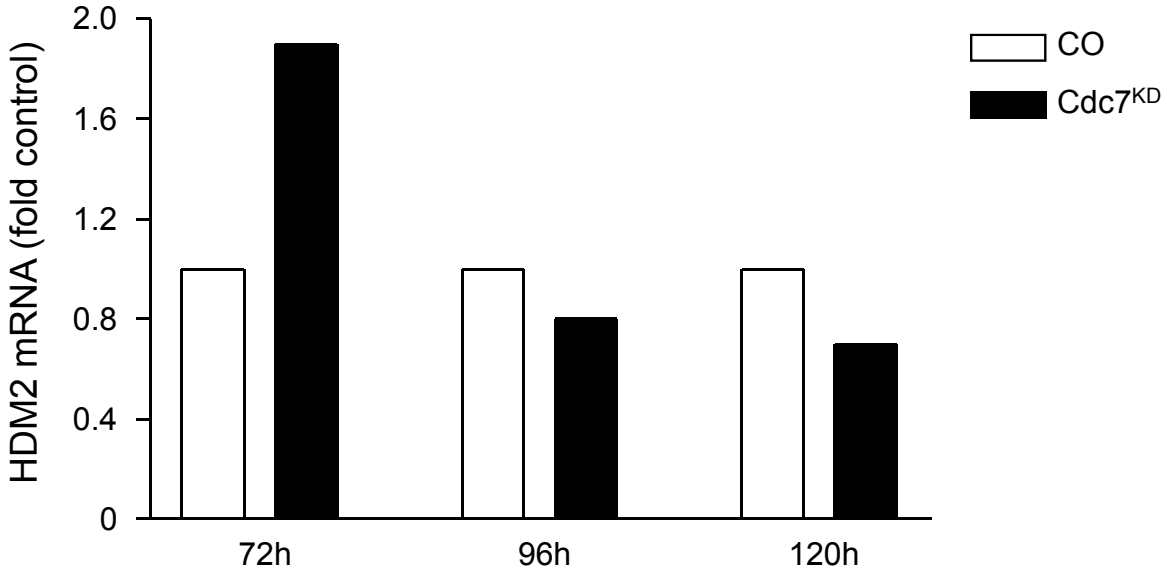

Supplementary Figure 8

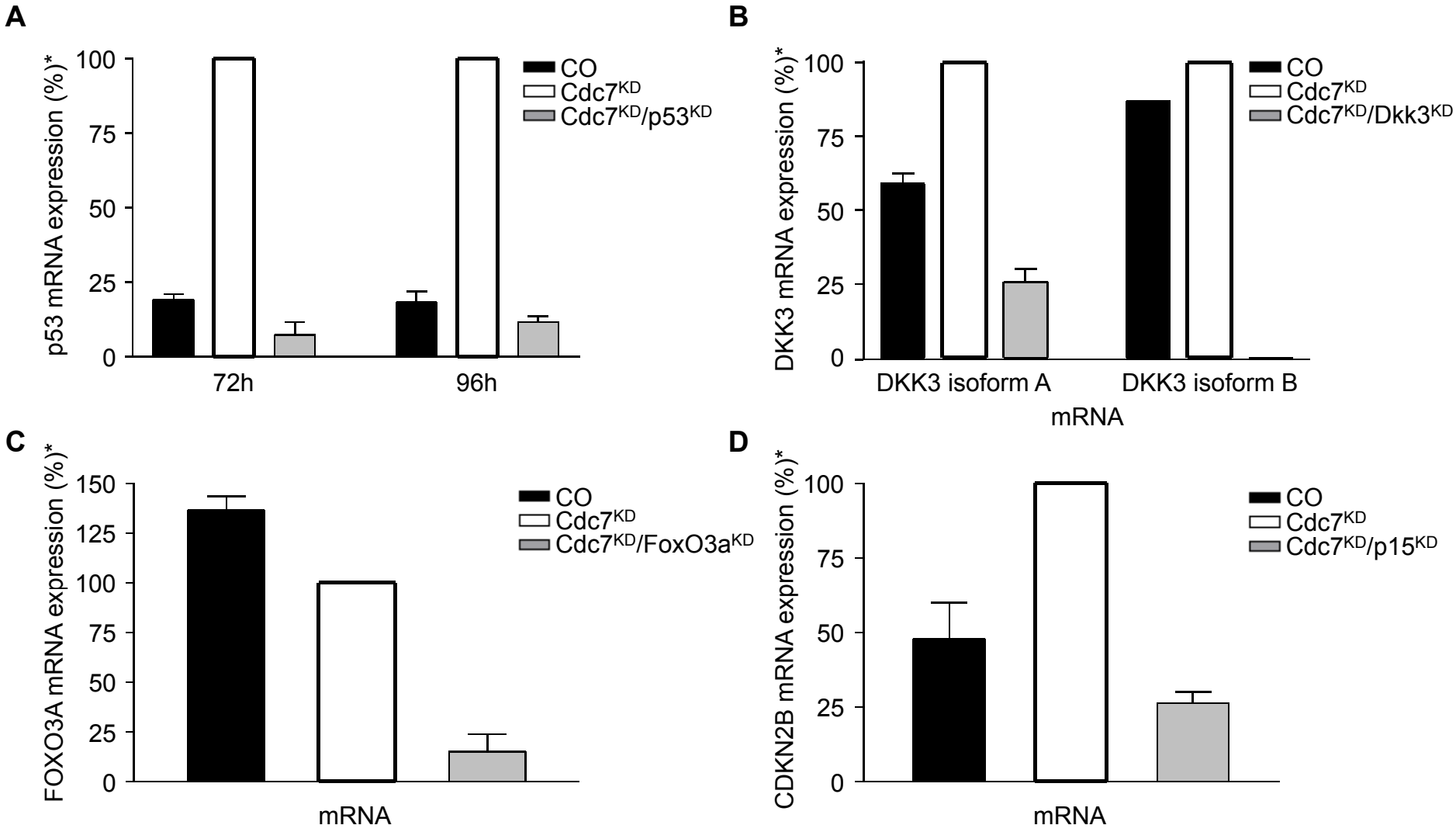

* mRNA level in Cdc7-depleted cells set as 100%

Supplementary Figure 9

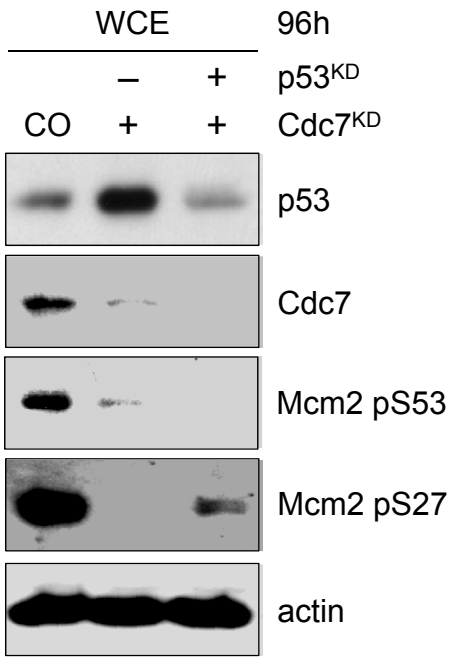

Supplementary Figure 10

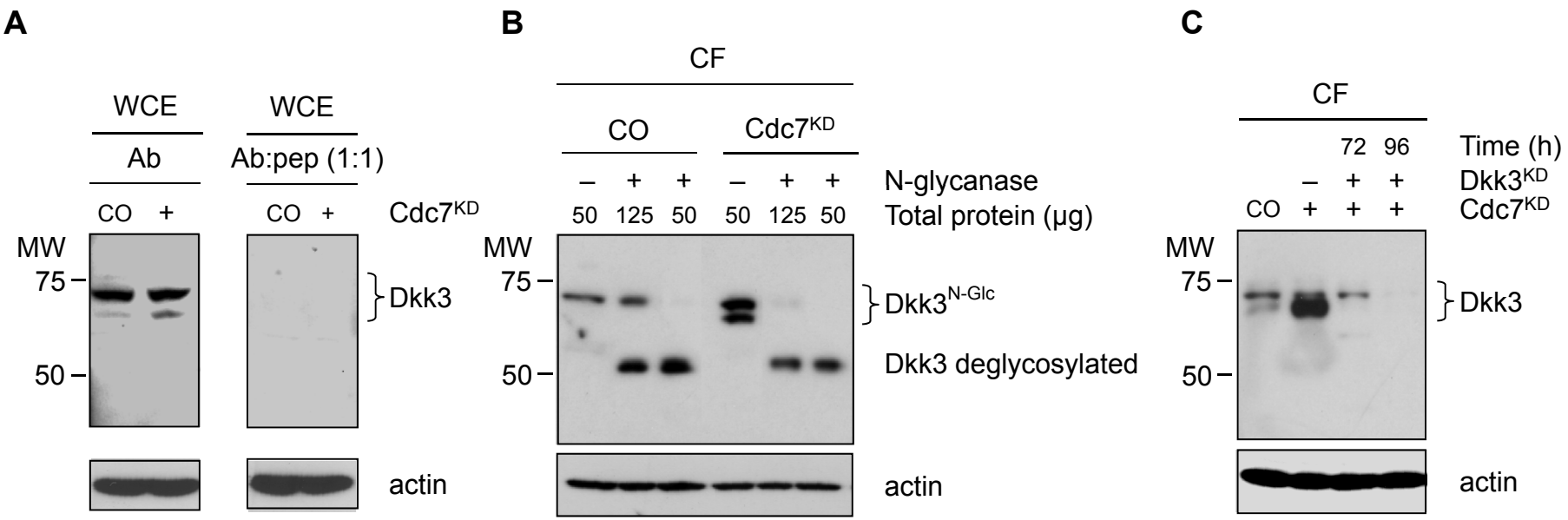

Supplementary Figure 11

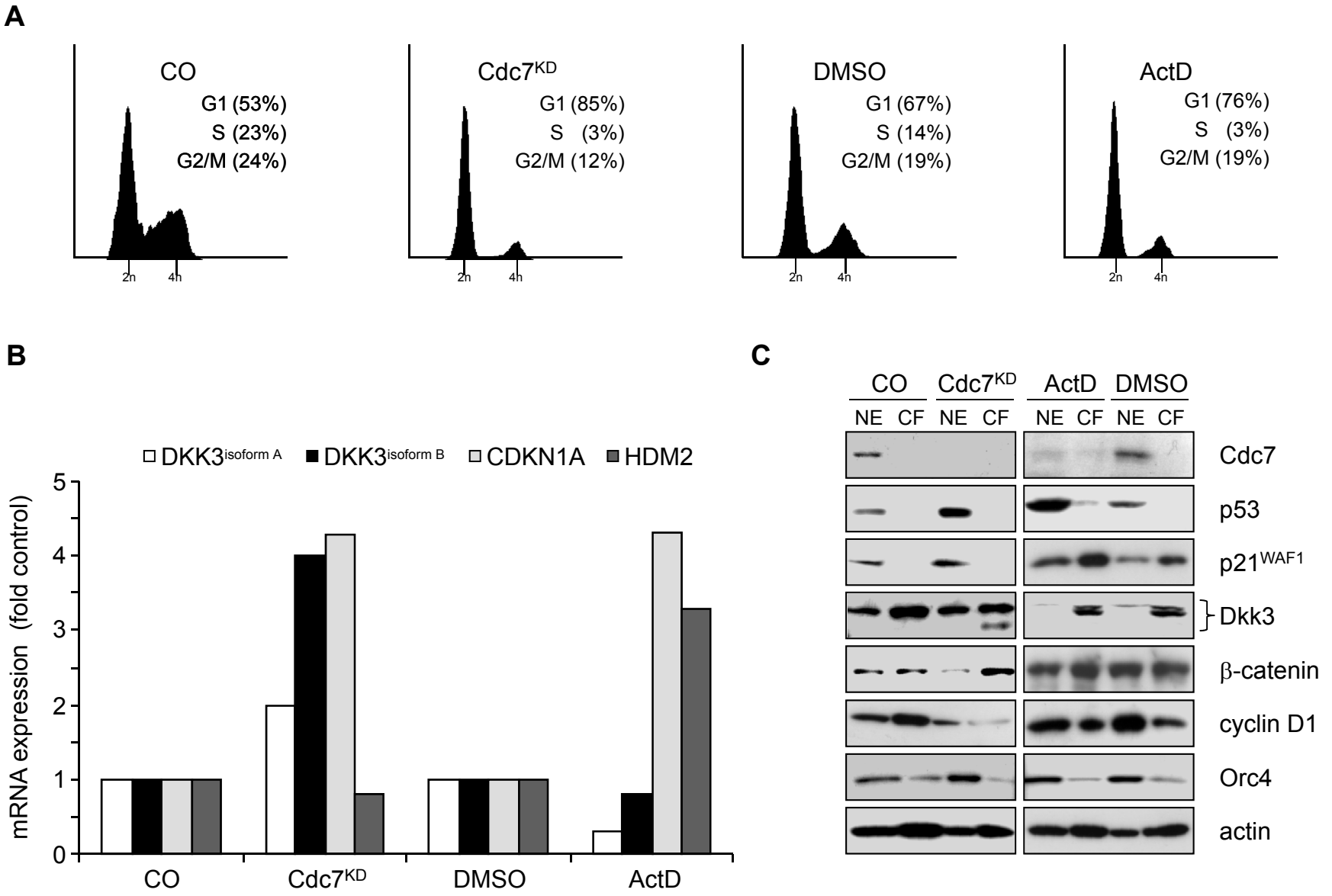

Supplementary Figure 12

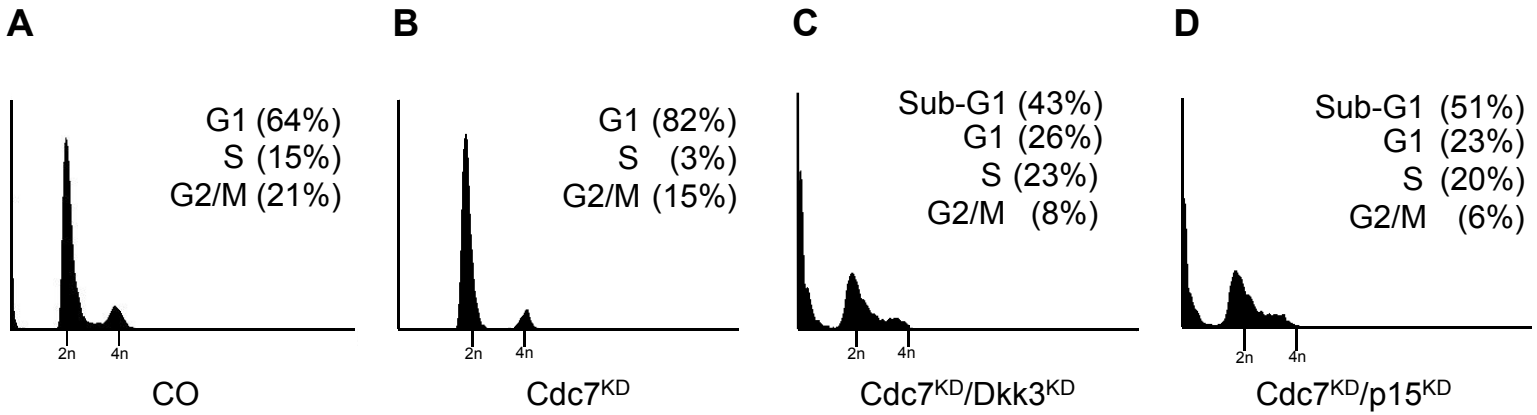

Supplementary Figure 13

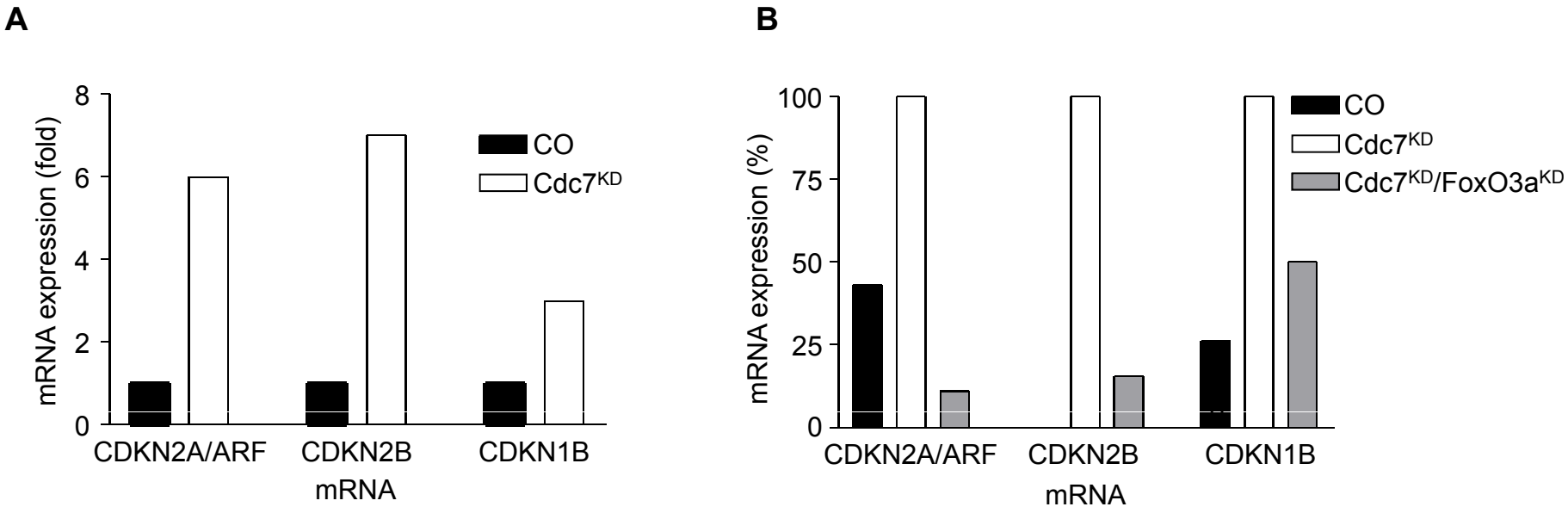

Supplementary Figure 14

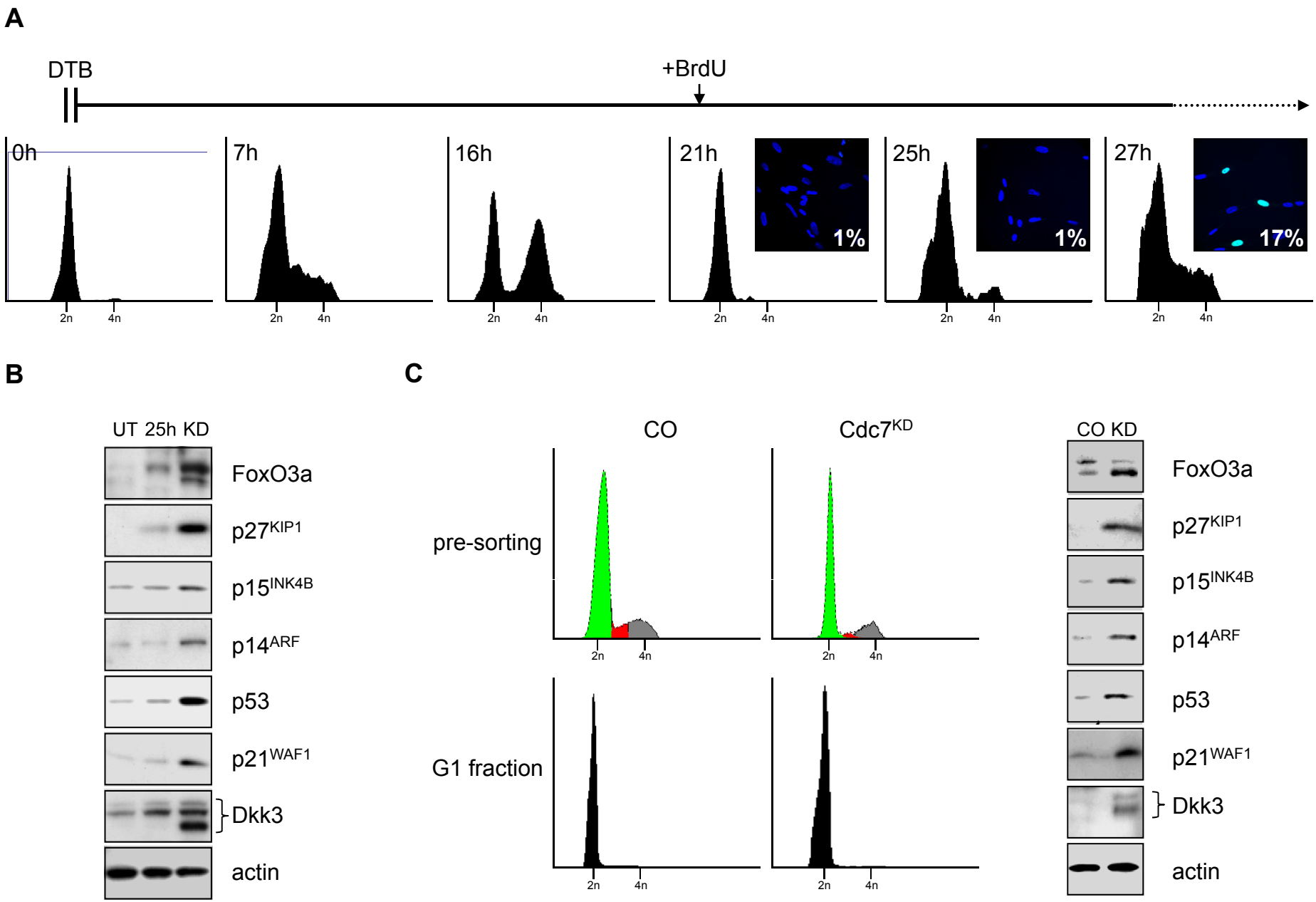

Supplementary Figure 15

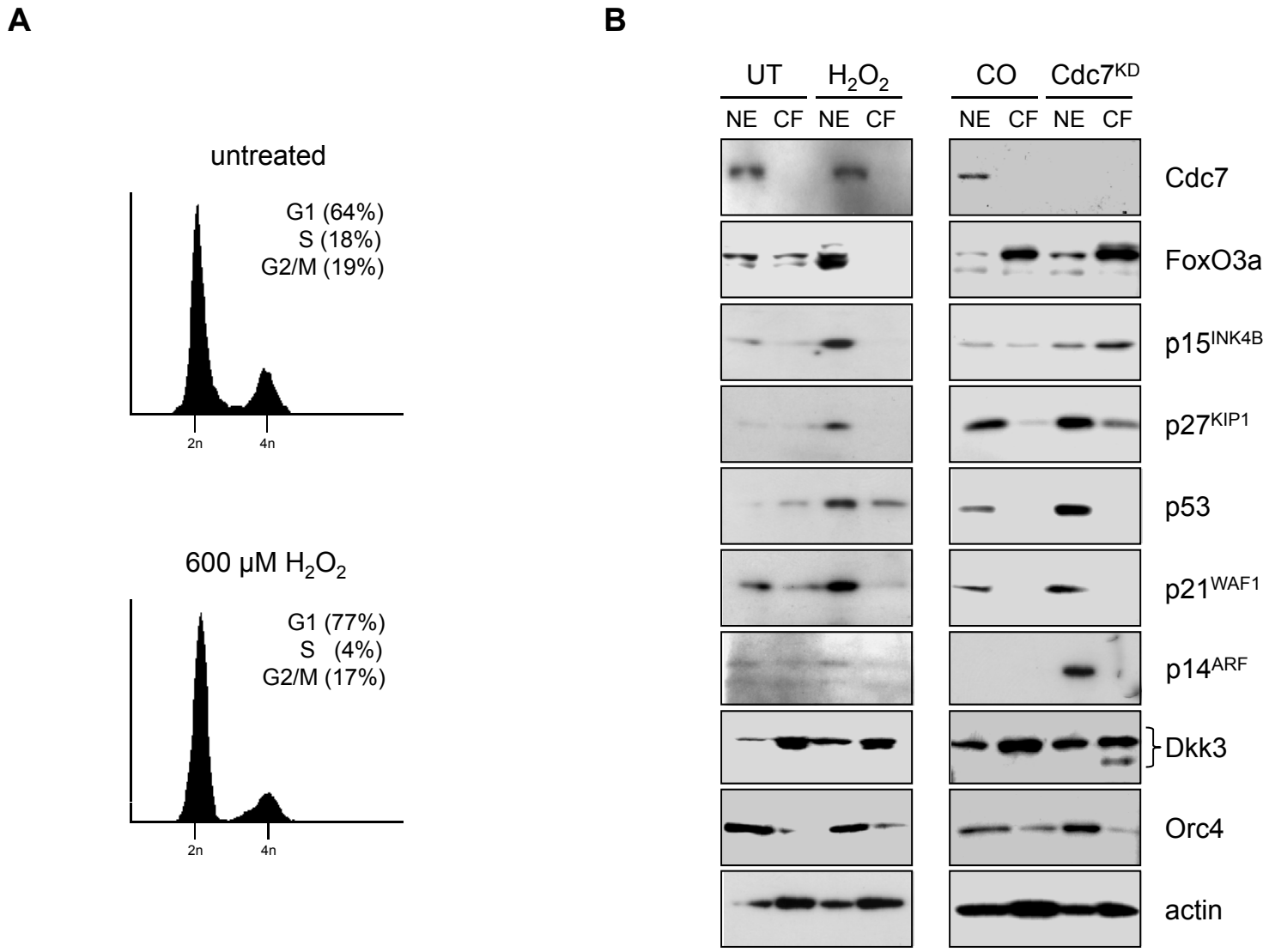

Supplementary Figure 16

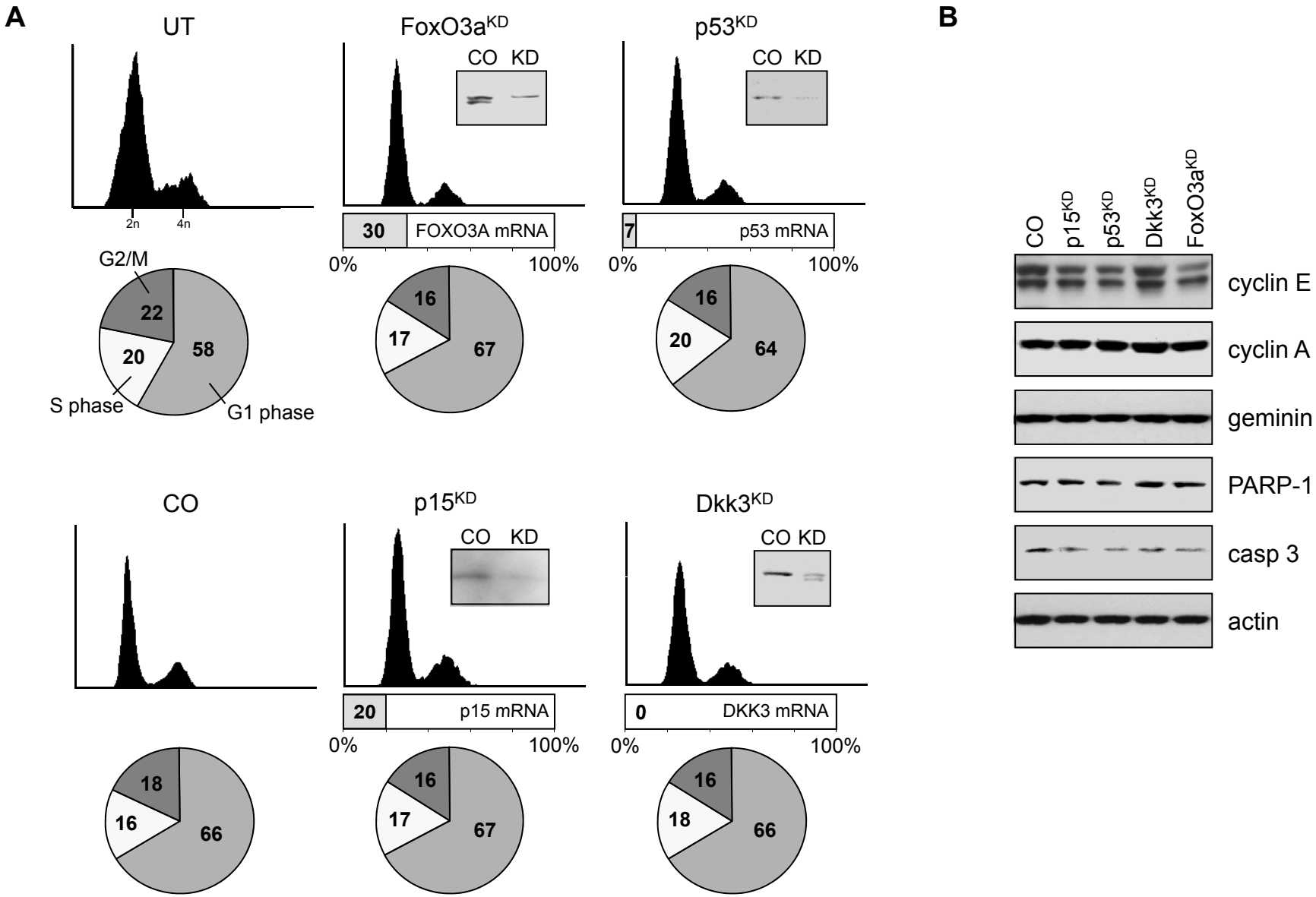

Supplementary Figure 17

A

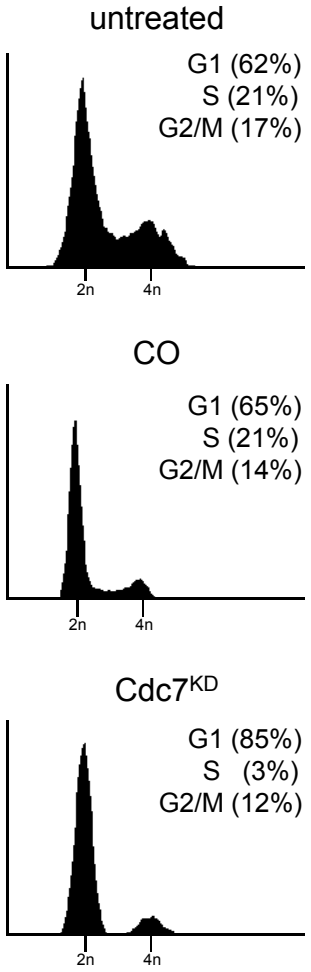

B

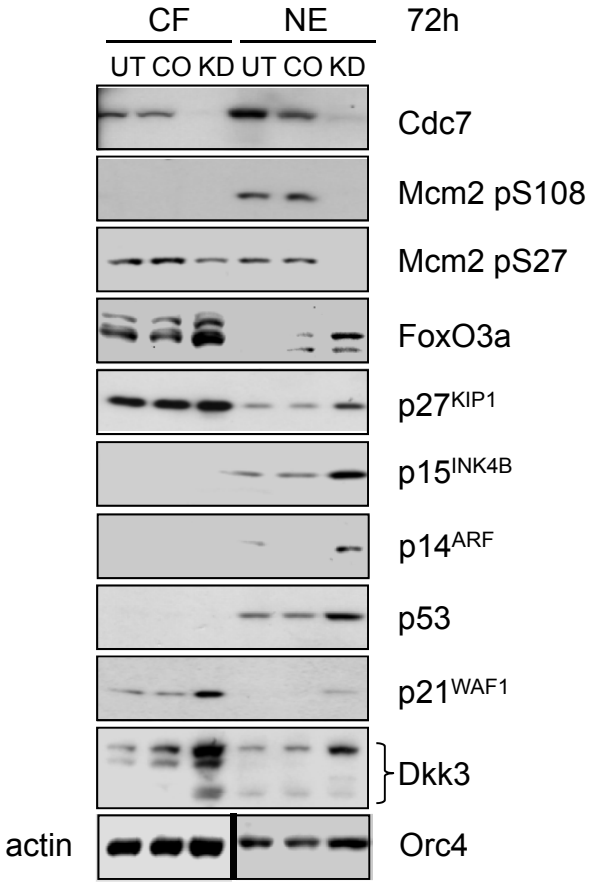

Supplementary Figure 18

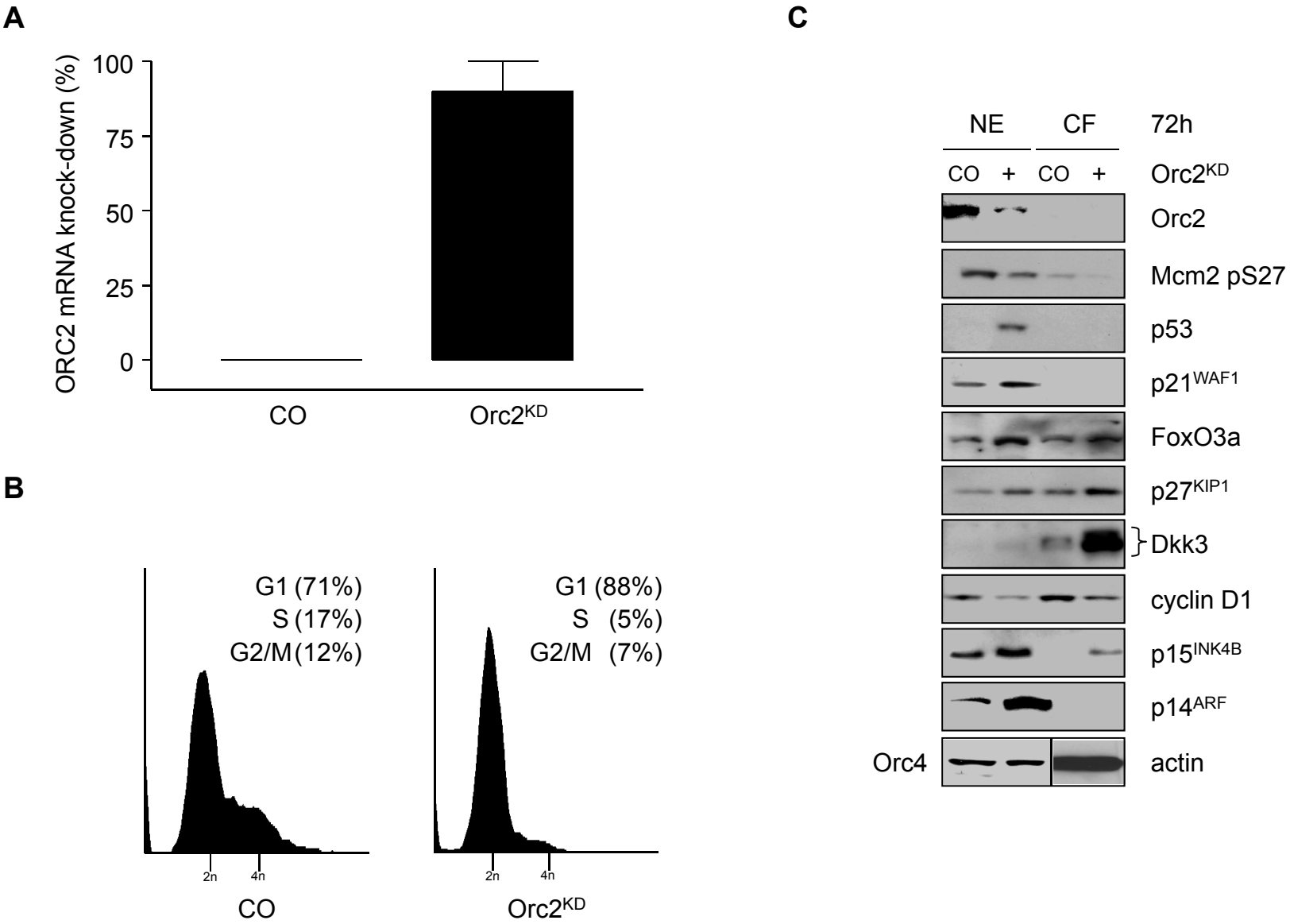

Supplementary Figure 19

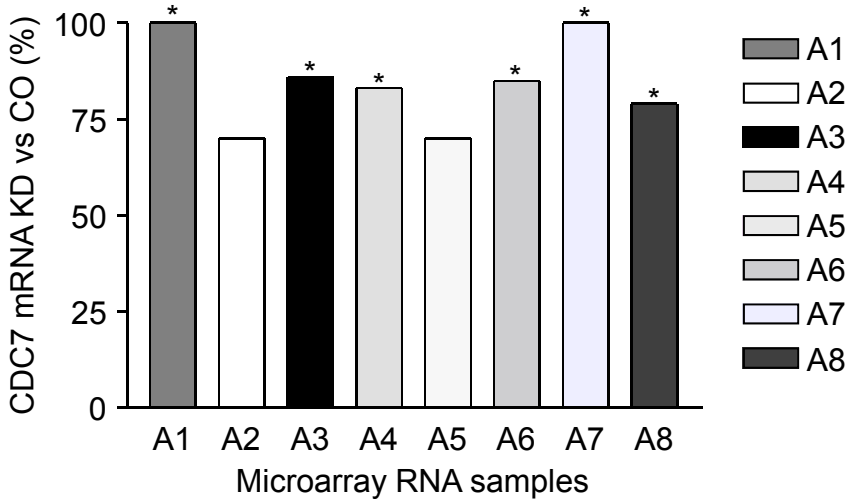

Supplementary Figure 20